2010

Numerical Investigation Of The Influence Of The Transient Flow Inside the Suction And Discharge Chamber On Heat Transfer Of A Small Reciprocating Compressor

Stephan Lehr
Technische Universitaet Dresden

Follow this and additional works at: http://docs.lib.purdue.edu/icec

Lehr, Stephan, "Numerical Investigation Of The Influence Of The Transient Flow Inside the Suction And Discharge Chamber On Heat Transfer Of A Small Reciprocating Compressor" (2010). *International Compressor Engineering Conference.* Paper 2028.
http://docs.lib.purdue.edu/icec/2028

Numerical Investigation Of The Influence Of The Transient Flow Inside the Suction And Discharge Chamber On Heat Transfer Of A Small Reciprocating Compressor

Stephan LEHR
Technische Universitaet Dresden,
Dresden, Germany
(stephan.lehr@tu-dresden.de)

ABSTRACT

The consideration of the convective heat transfer in the suction and discharge region of a compressor is handled differently in the literature. Commonly used are correlations for a steady state turbulent flow through a pipe like Chrustalev *et al.* (1998), Xin *et al.* (2000), Link *et al.* (2007). Here it is a point of principle whether such an approach is justified.

Subjects of the present work are the consideration of the suction and the discharge chamber of a small air brake piston compressor. Here the influence of the fluid flow on the heat transfer inside the suction and the discharge chamber was investigated by means of CFD simulations for different reed valve behaviours.
Three different working conditions for both the suction and discharge chamber are compared for low and high speed of the compressor:
a) steady state valve mass flow,
b) a mass flow for ideally opening and closing valve and
c) a mass flow in case of fluttering valves close to reality.

1. INTRODUCTION

The fluid flow in the suction chamber and the discharge chamber of the investigated air compressor can be seen as a turbulent flow. This is caused by the rotational speed and the intermittent process. Consequently an influence of the gas velocity on the heat transfer exists by forced convection inside the suction and the discharge chamber. In this presentation 750 min^{-1}, below named "low speed" and 2430 min^{-1}, below named "high speed" will be investigated.
On the one hand the before mentioned correlations for the heat transfer of a steady state turbulent flow in a pipe use a simple geometry. The suction and discharge chamber, in some cases with a complicated geometry, are handled as a pipe with an equivalent diameter. On the other hand the steady state mass flow is used. The steady state mass flow is the only (experimental) measurable value of mass flow in the compressor or compressor unit.

The influence of the transient behaviour caused by the intermittent operating condition of the compressor is unseizable that way. The higher the speed of the compressor is, the more far away from the maximum of the transient valve mass flow is the steady state mass flow. Furthermore the valve opening time is shorter. So the suction reed valve of the investigated compressor is opened about 40 percent and the discharge reed valve is opened about 10 percent of the work cycle time.

Also a higher frequency of the mass flow caused by the additional movement of the reed valve during the opening and closing process, so-called valve fluttering, can not be described by the steady state mass flow. The valve mass flow can increase and decrease strongly within a very short time and there will be no hint on this fact within the steady state mass flow! So we have to expect a very high velocity of the gas inside the chambers, but only temporary and localized.

The reed valve movement has been proven experimentally and is shown in Figure 1 for different speeds of the compressor. It is visible that the frequency of the suction valve movement is increased with decreased speed. So one can see that during the low speed cycle time of 80 ms the suction valve is twelve times closed or nearly closed, and during the high speed cycle time of about 24 ms this behaviour occurs five times. Because of the high pressure conditions in the discharge chamber it is not easy to measure the discharge valve behaviour by using the existing motion sensor system explained by Zosel (1999). For this reason this work contains no experimental discharge reed valve motion. But even at the discharge side such behaviour can be expected and

the question is: Is there an influence of the reed valve behaviour on the heat transfer inside the suction and the discharge chamber?
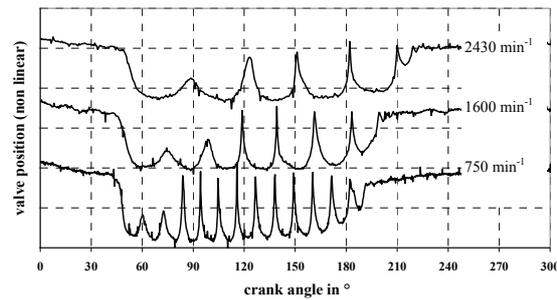

Figure 1: Suction valve movement (fluttering) – experimental data for different speeds

2. PROVIDING OF BOUNDARY CONDITIONS

For every numerical simulation boundary conditions are necessary. Here the surfaces of the domain of the suction and discharge chamber are considered as walls and are supposed to have a given temperature as boundary conditions. In this work, instead of a difficult to handle temperature distribution a special case of a constant temperature at every wall without any distribution on a wall will be considered. For low speed 120 °C and for high speed 190 °C for every suction and discharge chamber wall is used. These temperatures are based on experimental results.

The boundary conditions at the suction pipe are the ambient pressure (1 bar) and a constant suction gas temperature (60 °C). At the suction chamber valves the working condition a) a steady state valve mass flow, b) a mass flow for ideally opening and closing valve and c) a mass flow in case of fluttering valves close to reality will be provided. The discharge chamber valves also have steady or transient mass flow information depending on the working condition and temperature information as well. The discharge pipe is equipped with high the pressure condition (13.5 bar).

To generate the boundary conditions it is necessary to evaluate the transient working chamber states. In this work the existing experimental data of the p,V-diagram for low speed and high speed are modelled. To calculate the state inside the working chamber a zero-dimensional model for the thermodynamic state is used. Hence the local differences and the kinetic energy inside the working chamber are neglected and the fluid is considered as ideal gas. The reed valves are considered as a simple mass-spring model. Furthermore leakage and radiation is neglected, but convective heat flow inside the compressor chamber is included. The temperature of the cylinder liner is known from measurements and set to constant. The suction valve temperature as well. Also the pressure inside the suction and the discharge chamber is used from experimental data as a function of time. As a result of the calculation of the working chamber the mass flow at the suction and discharge valve is available and the working chamber temperature as well.

Criteria for a sufficient conformity between experimental data and the calculation are:
- the p,V- diagram from the experiment and the calculation are supposed to match well,
- the mass flow at the suction valve for the working cycle is supposed to be in agreement with the experimental mass flow,
- the qualitative suction valve motion is supposed to be in agreement with the experimental data.

To guide the calculation to steady state condition for every rotation the mass, the temperature and the pressure inside the working chamber are supposed to be in agreement between start and end of the calculation.

The results show that the valve motion agreement is good for low speed but for high speed only possible with a small displacement of phase. This is due to the limitation of the simple valve model. All other demands are fulfilled with good agreement.

A forced agreement is the agreement between the mass flow of the suction valve model of the steady state valve (experimental data), the ideally opening and closing of the valve and the fluttering of the valve:

$$\int_{0°}^{360°} \dot{m}_{steady} \cong \int_{0°}^{360°} \dot{m}_{ideal} \cong \int_{0°}^{360°} \dot{m}_{fluttering} \cdot \tag{1}$$

Figure 2 shows the results of the working chamber calculations of the mass flow models of the suction and discharge valve at low speed and high speed. The mass flow models in Figure 2 are only shown for the working time of the valves during the cycle.
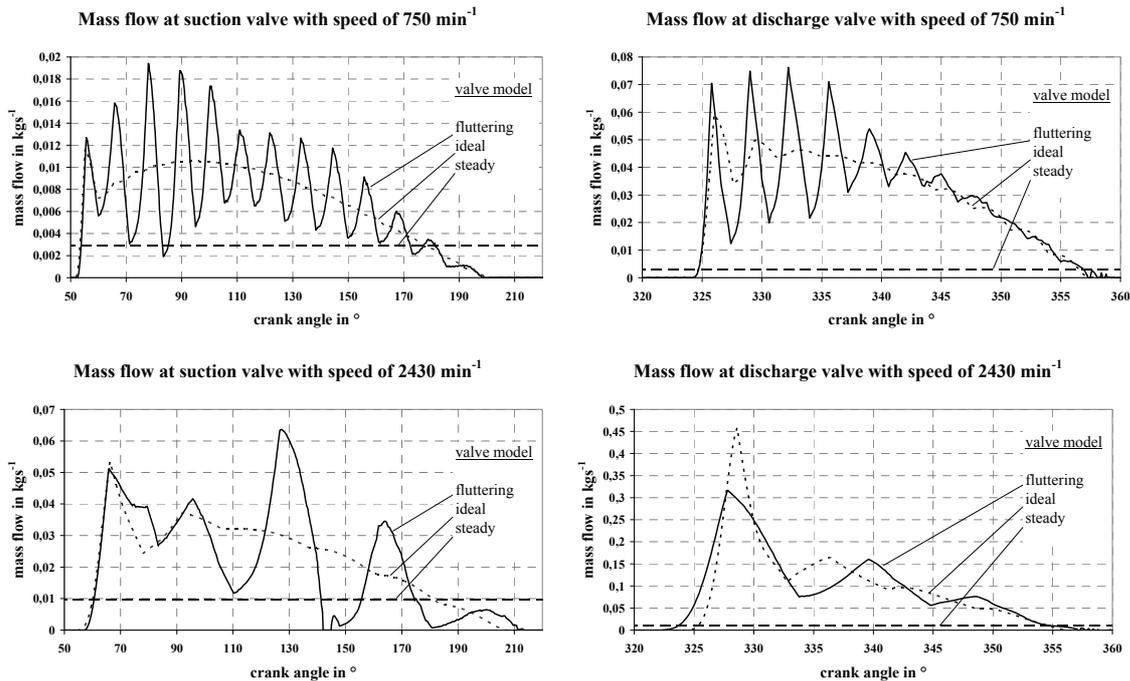
Mass flow at suction valve with speed of 750 min⁻¹

Mass flow at discharge valve with speed of 750 min⁻¹

Mass flow at suction valve with speed of 2430 min⁻¹

Mass flow at discharge valve with speed of 2430 min⁻¹

Figure 2: Mass flow models for the suction and the discharge chamber for rotational speed of 750 min⁻¹ and 2430 min⁻¹ as boundary condition for the fluid flow simulation

The mass flow of the fluttering suction valve and the fluttering discharge valve is – as one can expect from the information of Figure 1 – very different between low and the high speed. A certain backflow occurred in the calculation of the working chamber (suction valve, high speed, fluttering) but was neglected for the fluid flow simulation of the suction chamber.

Further there is quite a difference between the ideal valve and the fluttering valve because of higher frequency of the fluttering valve at low speed and high speed. The high speed discharge valve model of the ideal and the fluttering valve is at least very similar.

The also shown steady state mass flow from the experiment is for low speed 0.00293 kg/s and for high speed 0.00971 kg/s. Here the difference between the steady state model and the ideal respectively the fluttering model is very high for the discharge chamber at high speed and moderate for the suction chamber at low speed.

3. GEOMETRY SIMPLIFICATION OF THE SUCTION AND DISCHARGE CHAMBER

The simulation of the fluid flow is realized for the suction and the discharge chamber separately and without a consideration of the solid walls. The whole geometry is shown in Figure 3. The significant parts are labelled within the picture. For better understanding of the compressor size a common golf ball is placed in the area of the suction chamber.
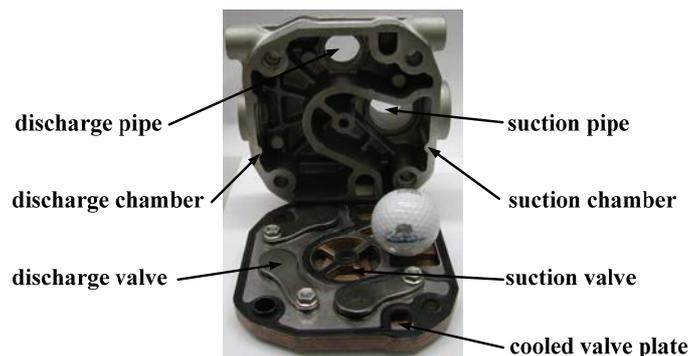
Figure 3: Cylinder head and valve plate of the investigated air brake compressor

For better results of the simulation mesh quality the geometry has been simplified. Figure 4 shows the original and modified geometry of the suction chamber and the discharge chamber. The modification is also labelled within the sketch.
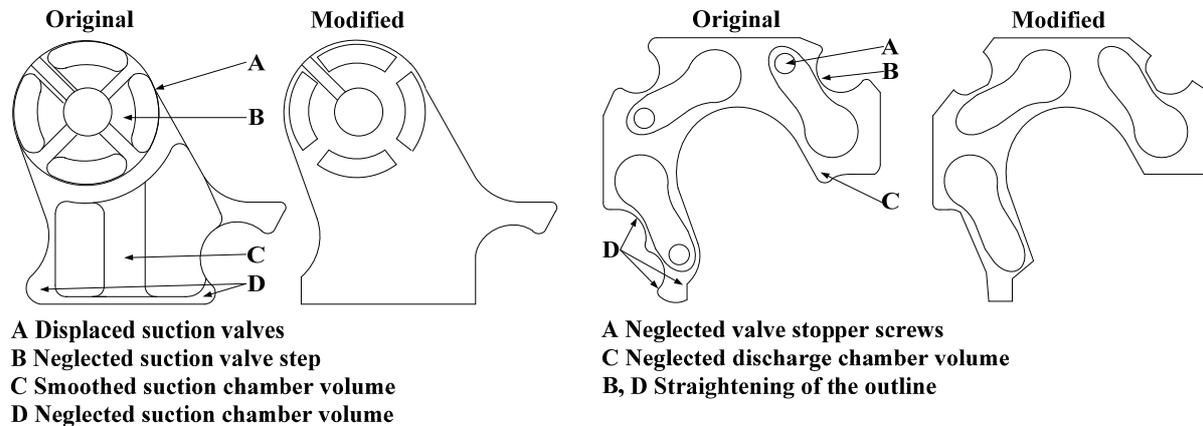

A Displaced suction valves
B Neglected suction valve step
C Smoothed suction chamber volume
D Neglected suction chamber volume

A Neglected valve stopper screws
C Neglected discharge chamber volume
B, D Straightening of the outline

Figure 4: Modification of the suction and discharge chamber geometry for CFX simulation

4. ARRANGEMENT OF AREAS FOR THE SUCTION AND DISCHARGE CHAMBER

The before mentioned walls of the suction and discharge chamber were split into different parts before the simulation mesh has been created. The reason is to provide the boundary conditions (temperature) and obtain detailed information of the wall heat flux. As a next step it is possible to estimate a heat transfer coefficient for every different part of the chamber geometry. The different parts can be seen in Figure 5 and 6 for the suction and discharge chamber.
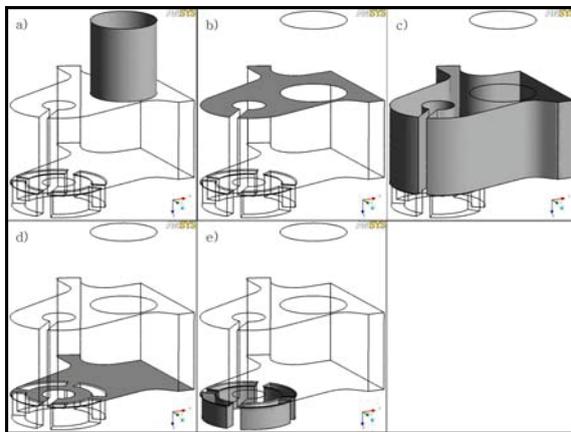

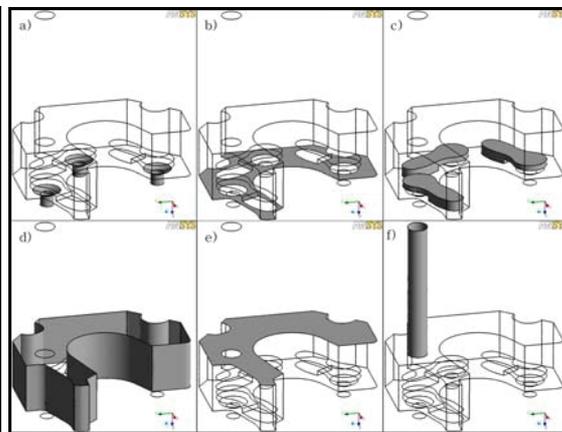Figure 5: Suction chamber surfaces

Figure 6: Discharge chamber surfaces

The surface of the suction chamber were split into the suction pipe (a), the suction chamber upside (b), the suction chamber side (c), as a shell, the valve plate (d) and the suction valve passage (e).
The surface of the discharge chamber has been split into the (three) discharge valve passage (a), the valve plate (b), the (three) valve stopper (c), the discharge chamber side (d), as a shell, the discharge chamber upside (e), and the discharge pipe (f).

5. DISCRETISATION AND SIMULATION

To discretize the geometry the commercial mesh generator ANSYS ICEM has been used. Both the suction and the discharge chamber are equipped with an unstructured mesh this way. For the fluid flow and the heat transfer consideration the boundary layer close to the wall is very important. Here this boundary layer is discretize with prism elements and contains 20 layers. So it is possible to avoid the wall function to calculate the heat transfer and switch instead to a direct calculation of the close-to-the-wall-layer. The geometry of the suction chamber and the discharge chamber contains more than 220.000 nodes. The same procedure was used in a work presented by Lehr *et al*. (2008).

The calculation has been realized by using a constant Courant number. So the time steps are not equidistant but minimized during the time the valves are open and enhanced during the times the valves are closed. The transient simulation has been carried out for low speed and high speed for the ideal valve and the fluttering valve. Here the simulation has been carried out for two revolutions for the suction chamber and for three revolutions for the discharge chamber. The results of the last revolution have been used for the presented results in this work.

For the steady state simulation with constant mass flow the simulation has been aborted after reaching constant values for the wall heat flux.

As main results of the simulation the wall heat flux at the different parts of the geometry, the mass flow at the valves and the temperature at the inlet and the outlet of the chambers are used.

6. RESULTS AND DISCUSSION

To estimate the heat transfer coefficient α for the suction chamber and the discharge chamber the examination of the wall heat flux results $\dot{q}$ take place by using the common Newton approach for convection:

$$\dot{q} = \alpha \cdot \left(T_{Wall} - T_{Gas} \right) \tag{2}$$

The wall temperature is set constant for all walls in every chamber and is different only between the simulation of the low and high speed conditions. So, as mentioned, a special case without temperature distribution of the suction and discharge chamber wall is used.

The gas temperature is available from the simulation for every time step at the chamber inlet and outlet, and is changed during the simulated revolution. So it is on the one hand possible to use these temperatures directly to create an average for the chamber temperature. On the other hand it is possible to use an averaged temperature for the gas inlet and outlet. It is a general question to choose the "right" temperature difference to express the heat transfer coefficient. In this work a mass flow averaged temperature for the gas at every inlet and outlet is used. So one is able to use these temperature values, especially at the discharge valves, to provide the inlet temperature information for the steady state simulation. For the suction pipe this procedure is not necessary. This temperature is constant for every simulation of the suction chamber.

The evaluation of the mass flow averaged temperature is shown in equation (3) using the example of the discrete simulation results of the suction valve $\overline{T}_{sv}$:

$$\overline{T}_{sv} = \frac{1}{m_{sv}} \cdot \sum_{i=1}^{n} T_{sv,\,i} \cdot \dot{m}_{sv,\,i} \cdot \left(\tau_i - \tau_{i-1} \right) \quad . \tag{3}$$

Therein the temperature at the suction valve $T_{sv,\,i}$, the mass flow at the suction valve $\dot{m}_{sv,\,i}$ and the simulation time τ_i is known for every simulation step i. The total mass at the suction valve m_{sv} is the sum of the discrete mass flow results for all time steps:

$$m_{sv} = \sum_{i=1}^{n} \frac{\dot{m}_{sv,\,i} + \dot{m}_{sv,\,i-1}}{2} \cdot \left(\tau_i - \tau_{i-1} \right) \quad . \tag{4}$$

This, now fix, temperature has been used as one reference value for the revolution at the suction chamber outlet. For the temperatures of the discharge valve $\overline{T}_{dv}$ and the discharge pipe $\overline{T}_{dp}$ the same procedure is used. One mass flow is used for the discharge valve and for the discharge pipe.

The averaged gas temperature of the suction chamber $\overline{T}_{sc}$ and the discharge chamber $\overline{T}_{dc}$ is the arithmetical average between the inlet and the outlet temperature of the discharge and suction chamber. Now the heat transfer coefficient for every time step has been calculated at every wall of the suction and the discharge chamber by using equation (2). The results shown in Figure 7 are a summary by using an area averaged value of the heat transfer coefficient for a chamber, instead of presenting every single value, for a clearer display. Every diagram of Figure 7 contains the area averaged heat transfer results for one chamber with one speed and three mass flow conditions. The arrangement of the results can be compared directly with the mass flow conditions in Figure 2.
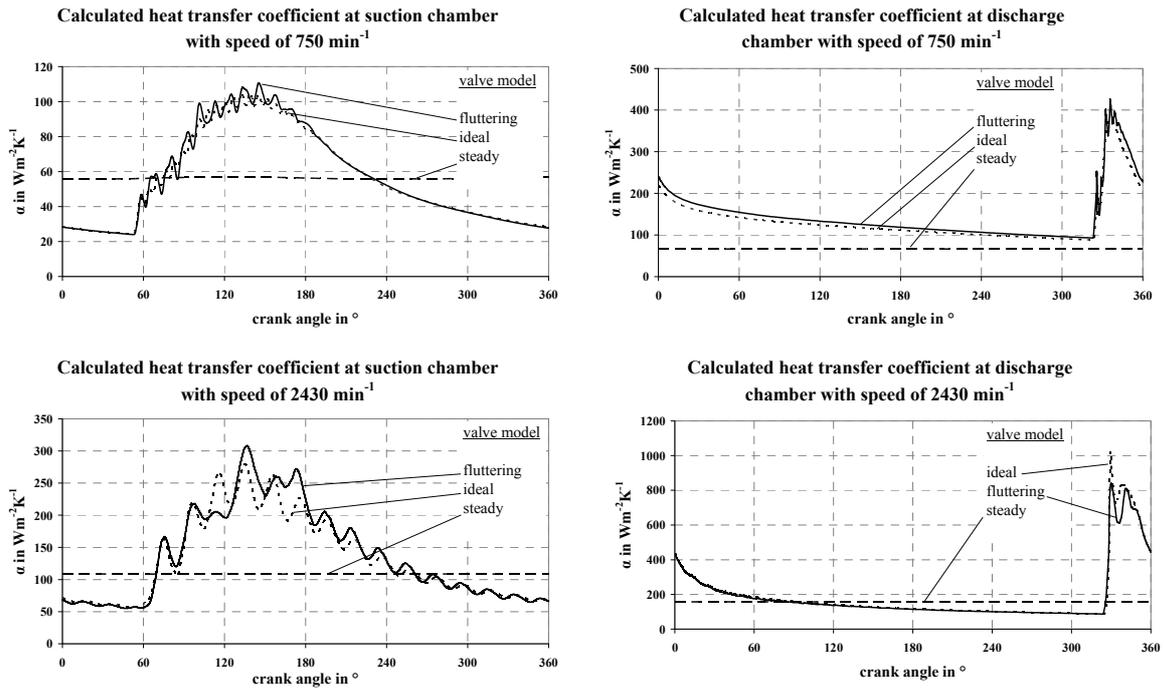
Figure 7: Results of the area averaged heat transfer coefficient of the fluid flow simulation for different mass flow model, speed and chamber

The results of the suction chamber at low speed for the fluttering valve model show a pulsation as one can expect from the mass flow. The pulsation is fading away shortly after the closing of the suction valve. The heat transfer coefficient decreases during the revolution and reaches the lowest point right before the valve is opened again. The results of the ideal and fluttering model are very similar with one exception: the pulsation amplitude. The result of the steady state heat transfer coefficient is of course constant and at moderate magnitude.

The results of the suction chamber at high speed show similar results and a pulsation for both the ideal and fluttering valve model but with a small phase displacement. Here the pulsation exists until the end of the revolution. So the flow inside of the chamber is in motion even after the end of the open-close-movement of the suction valve. The steady state heat transfer result is at moderate magnitude as well.

The results of the area averaged heat transfer coefficient in the discharge chamber at low speed show a pulsation with high amplitude but only for a short time. Also here the difference between ideal and fluttering model is negligible. The heat transfer coefficient is extremely different during the revolution. After an abrupt rise the results decrease for the rest of the revolution. The steady state results are below any result of the transient valve models.

The pulsation in the discharge chamber at high speed shows a 200 $Wm^{-2}K^{-1}$ lower peak of the heat transfer coefficient compared to the ideal valve model. A significant influence of the mass flow on the heat transfer coefficient can be seen at the ideal opening valve but just for a short moment at 329 ° crank angle. The results are in general similar to the low speed results but about twice the magnitude. One difference is the cutting across of the transient and steady state results and the achievement of a nearly constant transient valve model value after 180 ° in opposite to the low speed results.

The transient area averaged results of the heat transfer coefficient can be illustrated as time averaged value for a better comparison. These values are shown in Table 1 for the suction chamber and in Table 2 for the discharge chamber at low speed and high speed.

Table 1: Calculated suction chamber heat transfer coefficient in $Wm^{-2}K^{-1}$ for different mass flow models – time and area averaged

suction chamber					
speed 750 min^{-1}			speed 2430 min^{-1}		
steady	ideal	fluttering	steady	ideal	fluttering
56.3	56.4	57.0	108.5	132.4	137.0

Table 2: Calculated discharge chamber heat transfer coefficient in Wm^{-2}K^{-1} for different mass flow models – time and area averaged

discharge chamber						
speed 750 min^{-1}				speed 2430 min^{-1}		
steady	ideal	fluttering		steady	ideal	fluttering
66.5	136.4	146.5		157.5	195.7	189.2

The time and area averaged results of the simulation show one trend – an increase with enhanced convergence to the real valve behaviour. An exception is the discharge chamber at high speed. Here the result for the ideal valve model is already greater than for the fluttering valve model. The difference between the ideal opened valve model and fluttering valve model is small and independent of the speed and the considered chamber. The differences between the three investigated models are very small at low speed considering the suction chamber and large considering the discharge chamber.

After the simulation of the steady state and transient mass flow models a correlation from the standard literature for heat transfer in a pipe has been investigated. Using the steady state mass flow of the low speed and high speed condition and the correlation for a turbulent flow through a pipe (equation (5), Hausen) it is possible to calculate a heat transfer coefficient by using a simple correlation.

$$Nu = 0.0235 \cdot \left(Re^{0.8} - 230\right) \cdot \left(1 + \left(\frac{d}{L}\right)^{\frac{2}{3}}\right) \cdot \left(1{,}8 \cdot Pr^{0.3} - 0.8\right) \quad {}^{0.6 \le Pr \le 10^3}_{2300 \ \le Re \le 10^6} \tag{5}$$

Here the geometry of the suction chamber and the discharge chamber is represented by an equivalent diameter d of 52 mm respectively 82 mm. This diameter d is calculated by d = 4·A/U using the cross flow surface A, and the perimeter U of a chamber. The length L is 60 mm. The results are listed in Table 3 for the suction chamber and Table 4 for the discharge chamber at low and high speed.

Table 3: Comparison between steady state simulation and literature correlation for the suction chamber heat transfer coefficient in Wm^{-2}K^{-1}

suction chamber				
speed 750 min^{-1}			speed 2430 min^{-1}	
steady	equation (5)		steady	equation (5)
56.3	9.4		108.5	32.6

Table 4: Comparison between steady state simulation and literature correlation for the discharge chamber heat transfer coefficient in Wm^{-2}K^{-1}

discharge chamber				
speed 750 min^{-1}			speed 2430 min^{-1}	
steady	equation (5)		steady	equation (5)
66.5	! Re < 2300		157.5	16.1

The result of this correlation with the chosen conditions for the geometry and mass flow lead to a heat transfer coefficient in the magnitude of free convection for low speed and approximately three times higher for high speed inside the suction chamber. For the discharge chamber the calculated heat transfer coefficient at high speed lead to a value in the magnitude of free convection as well. Here the fluid flow does not reach the conditions of turbulent flow for the low speed mass flow! So this correlation can not be used. Using now a correlation for laminar flow would be absurd for a compressor discharge chamber at 750 min^{-1}.

One possible explanation for these steady state correlation results for the heat transfer in a pipe so far away from the steady state simulation of this work seems to be the neglect of the real geometry by the simple correlation. So it is not possible to consider a complicate geometry (Figure 5 and 6, valve, suction pipe, discharge pipe) and in this way a local increase of the velocity inside the chamber. Additionally the discharge chamber contains with the valve stopper a geometry which is completely not to consider by a correlation for a pipe.

7. CONCLUSION

The influence of different working conditions of the suction reed valve and the discharge reed valve on the heat transfer coefficient has been investigated by means of CFD simulations. Here three different conditions – a

steady state valve mass flow, a mass flow for ideally opening and closing valve and a mass flow in case of fluttering valves close to reality – have been investigated for the suction chamber and the discharge chamber for low speed and high speed of a small air brake reciprocating compressor.

The results illustrate that the difference between the ideal and the fluttering valve model is negligible for the heat transfer consideration inside the chambers. Even for the strong valve mass flow variation of the suction chamber at low speed (see Figure 2), the effect on the heat transfer coefficient is in a very small range – and this is unexpected, at least for the author. The transient simulation results of the heat transfer coefficient reach the maximum of more than 800 $Wm^{-2}K^{-1}$ at high speed in the discharge chamber. In general the results for the steady state simulation of the flow the heat transfer coefficient are cutting the transient results – except the discharge chamber at low speed.

A comparison of the steady state simulation results with a common approach for a steady state turbulent flow through a pipe is "not successful". The correlation for a tube leads to a completely different magnitude of the heat transfer coefficient. For the investigated case the results of the heat transfer coefficient for the steady state mass flow for low speed and high speed are far away from the simulation results and in the range of free convection. For this one can see on the one hand the mapping of the chamber geometry as simple pipe geometry. Furthermore other parts of the geometry are completely unconsidered using such an approach. On the other hand the influence of the time-dependent mass flow is not considered. So we can not expect realistic results from a simple correlation for a pipe. As shown in the presented work it seems to be more realistic too use a more sophisticated approach.

REFERENCES

Chrustalev, B.S., Krasnikov, A.G., 1998, Analysis of non-stationary processes of heat and mass exchange in the reciprocating compressor suction system for natural gas compression, International Compressor Engineering Conference at Purdue, West Lafayette, Indiana, USA

Xin, R., Hatzikazakis, P., 2000, Reciprocating compressor performance simulation, 15th International Compressor Engineering Conference at Purdue, West Lafayette,

Link, R., Deschamps, C.J., 2007, Numerical Modeling of the start up transient in reciprocating compressors, The 22nd IIR International Congress of Refrigeration, Beijing, China

Zosel, P., 1999, Kapazitives Messen von Bauteilbewegungen an Kolbenmaschinen, Zeitschrift Industriepumpen + Kompressoren, Heft 3, September 1999

Lehr, S., Langebach, R., 2008, Improvement of the volumetric and isentropic efficiency due to modifications of the suction chamber, International Compressor Engineering Conference at Purdue, Proceedings Vol.1, ID1129, 2008